

Improving the Sensitivity of Grating-echo Atom Interferometers for Measurements of Gravity

G. Carlse, J. Randhawa, A. Pouliot, T. Vacheresse, E. Ramos, A. Carew, and A. Kumarakrishnan*
Department of Physics and Astronomy, York University, Toronto, Ontario, Canada M3J 1P3

ABSTRACT

Precision measurements of gravitational acceleration g have far reaching applications in navigation and sensing as well as for tests of general relativity. Grating-echo atom interferometers (AIs) utilize simple setups and distinctive excitation schemes that involve a single excitation laser, and do not require velocity selection. They have demonstrated measurements of gravity precise to 75 parts per billion (ppb) by dropping laser-cooled atomic samples through ~ 1 cm. Here we describe progress toward realizing a cold atom gravimeter using an echo AI designed for drop heights of ~ 30 cm. The experimental technique involves illuminating the falling sample of laser-cooled rubidium atoms with two standing wave (sw) pulses separated by time $t = T$. The sw pulses are composed of two traveling-wave components, each having a wave vector of magnitude $k = 2\pi/\lambda$. Momentum state interference produces one-dimensional density gratings with a period $\lambda/2$ immediately after each excitation pulse. These gratings dephase due to the velocity distribution of the sample along the sw axis. The AI uses an echo technique to cancel the effect of velocity dephasing and observe a rephased density grating in the vicinity of the echo time $t = 2T$. The grating contrast and phase are measured by coherently backscattering a traveling wave readout pulse from the sample. The grating phase, measured with respect to a vibrationally stabilized inertial reference frame, scales as $2kgT^2$. A drawback of echo AIs is the signal-to-noise ratio, which is limited by the contrast of the grating and systematic effects due the refractive index of the sample. Here, we review improvements to the experimental design and investigate methods of improving the signal-to-noise ratio by optimizing the atom-field coupling. We describe progress toward realizing our goals of increasing the grating contrast and the backscattered signal. The improved contrast is expected to allow the experiment to be carried out at a lower density to reduce corrections due to the refractive index. We discuss a variety of excitation schemes for achieving a target precision of a few ppb.

Keywords: Precision Metrology and Quantum Sensors, Atom Interferometry, Coherent Transient Effects, Laser Cooling and Trapping of Neutral Atoms, Precision Measurements, Experimental Atomic Physics, Auto-locking Laser Systems, Atom Optics, Inertial Effects, Gravimeters, Photon Echoes, Laser Spectroscopy

1. INTRODUCTION

Laser-cooled atoms consisting of dilute, slow-moving gases are sensitive probes of gravitational forces. Atom interferometers (AIs) rely on the wave nature of cold atoms and precise control of matter waves by pulses of laser light that act as beam splitters and mirrors. In this manner, the roles of light and matter are interchanged in comparison with falling corner cube optical interferometers developed for geophysical exploration of natural resources that use optical elements to split and recombine light. The sensitivity of AIs is enhanced by increasing the enclosed area of space-time paths of atomic waves and by observing interference effects on extended, transit time-limited time scales of atoms through laser beams. Here, we discuss the development of a simple and distinctive single state, grating echo AI that utilizes ultracold samples of laser cooled atoms. We review the progress of measurements in a vibrationally stabilized, non-magnetic apparatus that are based on improving the signal-to noise ratio [1].

2. METHODOLOGY AND PROGRESS

The single-state grating echo AI has used laser-cooled Rb atoms for precision measurements of the atomic recoil frequency (which is related to the atomic fine structure constant α) and gravitational acceleration g [2-5]. This AI uses a single excitation laser, does not require velocity selection, and offers reduced experimental complexity in comparison to Raman

AIs. Laser-cooled rubidium atoms are excited along the vertical axis by two standing waves (sw). The sw pulses each carry a momentum corresponding to the wave vector k ($k = 2\pi/\lambda$, where λ is the wavelength of light) and are separated by a time T . After the first pulse at $t = 0$, atoms in the internal states of a single ground state manifold are diffracted into a superposition of momentum states separated by $2\hbar k$. The atomic wave function develops a recoil modulation on a time scale $\tau_q = \pi/\omega_q$ ($\sim 32 \mu\text{s}$), where $\omega_q = 4\hbar k^2/2m_{\text{atom}}$. Since this time scale is larger than the dephasing time T_D ($\sim 5 \mu\text{s}$) of the Doppler-broadened sample (temperature $\sim 2 \mu\text{K}$), the AI uses an echo technique to cancel the effect of dephasing and observe the recoil modulation: a second sw pulse applied at $t = T$ produces interference of momentum states separated by $2\hbar k$ near the echo time $t = 2T$ and creates a rephased density grating. The grating contrast and phase are measured by applying a near-resonant traveling wave read-out pulse, to detect the amplitude and phase of the coherently backscattered echo signal. The phase of the falling grating scales as gT^2 , and its precise measurement as a function of the pulse separation, T , is used to determine g .

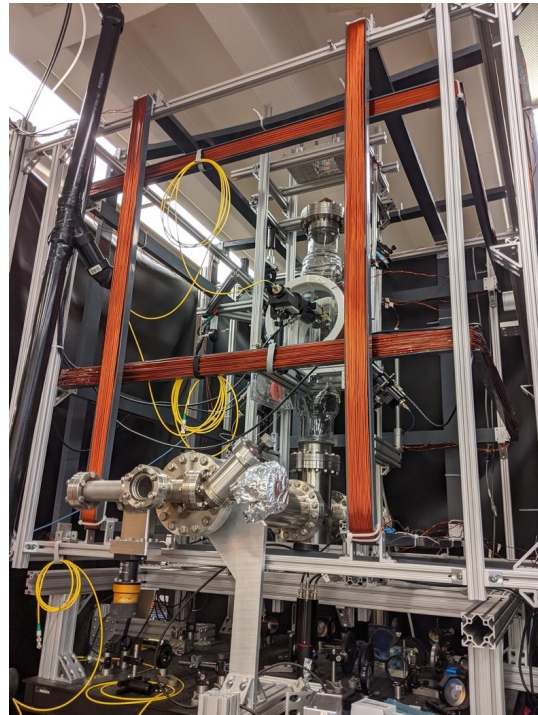
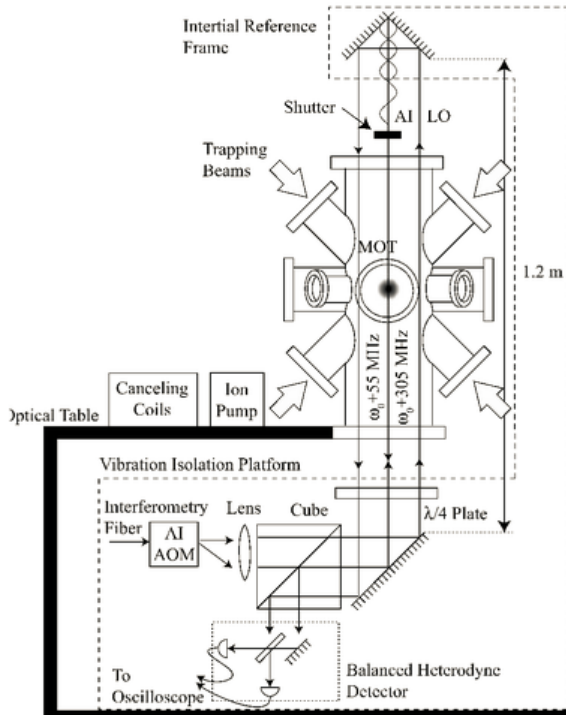


Figure 1: Experimental Setup (From references. [2,3])

Figure 2: Improved Experimental Setup

Phase 1: In the initial phase, the experiment used a Ti:Sapphire laser is used to generate light for atom trapping and interferometry using a chain of acousto-optic modulators (AOMs) that serve as frequency shifters and amplitude modulators. All these elements were placed on a pneumatically supported optical table. Light from these AOMs was transported to the atom trap using angle-cleaved, anti-reflection (AR) coated optical fibers. The vacuum chamber used for atom trapping was made of 316 L stainless steel and anchored to a separate optical table mounted on pneumatic vibration isolators as shown in Figure 1. The chamber was maintained at 5×10^{-9} Torr by an ion pump with a pumping speed of 270 L/s located 1 m away to reduce ambient magnetic fields. The chamber was surrounded by three pairs of magnetic field and gradient cancelling coils. A separate set of tapered coils wound on the chamber provided the magnetic gradient for atom trapping. The trapping optics, vacuum chamber, anti-Helmholtz and cancellation coils, and ion pump was supported by the optical table. The magneto-optical trap (MOT) was loaded from background vapor, with approximately 5×10^8 atoms loaded in 1 second. Time-of-flight charge-coupled device (CCD) camera images of atoms released after molasses cooling showed that the typical sample temperature was $20 \mu\text{K}$. The fiber-coupled beam used for atom interferometry was aligned through a single-pass AOM operating at 250 MHz. The circularly polarized diffracted beam from this AOM, which was directed along the vertical and used for excitation of atoms, was detuned 55 MHz above resonance. This beam was retro reflected through the atom cloud by a corner-cube reflector to produce sw excitation. The undiffracted beam, with a frequency of 305 MHz above the atomic resonance was spatially separated from the excitation beam by 2.5 cm. It was

aligned through the same optical elements as the excitation beam to minimize the impact of relative phase changes due to vibrations and serves as a local oscillator (LO). The LO was physically displaced upon reflection by the corner-cube. The background light entering the apparatus during the AI pulse sequence was minimized by pulsing a gate AOM only when the AI AOM is turned on. The excitation and LO beams were combined on a beam splitter and a balanced heterodyne detector with two oppositely biased Si photodiodes with rise-times of 1 ns. These detectors were used to record a beat signal at a frequency of 250 MHz. During the read-out pulse, the retro-reflection of the excitation beam was blocked by a mechanical shutter with an open/close time of 1 ms.

The corner-cube reflector, AI AOM, balanced detector, and related optics were anchored to a vibration isolation platform with a resonance frequency of 1 Hz, which rests on the pneumatically supported optical table. The optical table is effective in suppressing vibration frequencies above 100 Hz, whereas the vibration isolation platform suppresses frequencies in the range of 1–100 Hz. The mechanical shutter was separately anchored to the ceiling of the laboratory to reduce vibrational coupling. In this setup, only critical components were passively isolated with the vibration isolation platform.

Digital delay generators with time bases controlled by a 10 MHz signal from a rubidium clock (Allan variance of 5×10^{-12} in 100 seconds) were used to produce radio frequency (RF) pulses with an on/off contrast of 90 dB to drive the AOMs. The time delays of optical pulses were controlled with a precision of 50 ps. The read-out pulse intensity is comparable to the saturation intensity of Rb atoms so that the entire echo signal envelope can be recorded without appreciably decohering the signal. This signal, which was measured as a 250 MHz beat note, was recorded on an oscilloscope with an analog bandwidth of 3.5 GHz and mixed down to DC using the RF oscillator driving the AI AOM to produce the in-phase and in-quadrature components of the back-scattered electric field. While the atom trap is loaded, an attenuated excitation beam was turned on to record a 250 MHz beat note. This measurement re-initialized the RF phase used to mix the signal down to DC at the beginning of each repetition of the experiment and ensured that the relative phases between the excitation beam and the LO are the same at the start of the experiment. Although the LO and AI beams were strongly correlated at the beginning of the experiment, the phase uncertainty progressively increased with the time scale of the experiment, and it could not be corrected mainly because the motion of the corner-cube reflector was not measured. The typical repetition rate of the experiment varied between 0.8–3 Hz. In this configuration, atoms were dropped through a height of 1 cm and measurements of g precise to 75 ppb were demonstrated [2, 3].

Phase 2: During this phase, the stainless-steel vacuum chamber was replaced by a homebuilt non-magnetic glass vacuum system as shown in Figure 2. The glass chamber reduced decoherence effects related to inhomogeneous magnetic fields produced by a stainless-steel vacuum chamber and improved the molasses cooling of the sample to achieve sample temperatures of $\sim 5 \mu\text{K}$. Large diameter, chirped excitation beams, eliminated the differential Doppler shift of the atom from the two components of the sw pulses and increased the transit time of the atoms in the beam. Heterodyne detection was replaced by vibrationally insensitive PMT detection. This setup was used to realize a measurement of the atomic recoil frequency precise to 37 ppb [4, 5].

Phase 3: The main limitation in the passively stabilized experiments was the lack of reference to a proper inertial frame. Since the interferometer's sw excitation beam were generated by retro-reflecting a traveling-wave beam from a corner-cube retroreflector in the gravity experiment, the phase of the sw excitation was linked to the position of the corner-cube with respect to Earth's gravity field. This means that during the experiment, there was an uncontrolled phase accumulation in the signal proportional to the drift of the position of the apparatus. This placed an upper limit on the possible time scale of experiments, which in turn limited the achievable precision. The vibration spectrum of the lab environment may have also contributed to aliasing effects for certain experimental repetition rates, as suggested by the data in Refs. [2,3]. As a result, the apparatus was further modified [6]. *A picture of this apparatus is shown in Figure 2.*

This new apparatus includes a high-precision accelerometer, attached to the corner-cube reflector to provide a more reliable reference of the experiment's frame of reference to the Earth's frame. The position of the reflector can be measured at the beginning of each experiment, and this data can be used to either post-correct the data, or to actively correct the frame of reference using a mechanical actuator, voice coil. The sensitivity of the interferometer to motion of the sw potential during the experiment can be calculated [7, 8] making it possible to achieve post-correction.

The apparatus is also passively isolated from ambient vibrations by a two-stage system. The first stage consists of a laminar flow pneumatic isolator, on which the optics table is mounted. This isolator has a vertical resonance around 1 Hz.

To further decrease the system's susceptibility to low-frequency vibrations, the atom trapping optics, AI optics, and vacuum chamber are mounted on a passively tuned spring damping system that has a sub 1 Hz vertical resonance. This isolator is, in turn, mounted on top of the previously mentioned pneumatic isolation system. The only components of the apparatus that are not mounted to the spring-based isolator are the field cancellation coils, and an ion pump due to the mass limit of this isolator. The coils and the pump are instead attached directly to the bottom of the pneumatically isolated table. Since the zero field/gradient region created by the cancelling coils is quite large compared to the expected motion of the apparatus due to vibrations, the mounting scheme for the coils is not expected to affect the stability of the measurements.

Since the AI relies on two traveling wave components to produce sw excitation, it is necessary to monitor the drift of the retro-reflecting mirror with respect to the other optics in the system using a Michelson-type interferometer and a far-off resonance probe beam. One arm of this interferometer includes the retro-reflecting mirror and the polarizing-cube beam splitter along the vertical excitation beam path and the output of the interferometer is recorded on a sensitive photodetector. The signal from the probe beam is used to post correct the AI phase measurement. Such a correction will account for the movement of the lower optics with respect to the retro-mirror. Since the retro-mirror's position with respect to Earth is monitored by a sensitive accelerometer, the phase of the sw excitation with respect to Earth will be fully determined. In an alternative scheme, the signal from the interferometer could be used to actively control the position of the retro-mirror with respect to the lower optics through the aforementioned voice coil and a PID control loop used in pioneering Raman AI experiments [9, 10].

Another shortcoming of the apparatus used in Phase 1 and Phase 2 related to the magnetic field canceling coils. In the absence of state selection, the presence of magnetic field gradients and magnetic field curvature in the vicinity of the atoms during the experiment results in an additional force, which cannot be separated from the gravitational force. As such, the available time scale for experiments was also limited by the incomplete magnetic field cancellation and the magnetization of the vacuum chamber. The cancellation was incomplete due to the non-optimal geometry of the field-canceling coils and the magnetization of the vacuum chamber. In brief, the B-field at the position of the atoms is canceled by 3 sets of mutually perpendicular coils. Optimal cancellation is obtained when each set of coils is arranged in a "Helmholtz" configuration, where the (circular) coils are separated by a distance equal to their radius. In our experiment, the coils were initially set up in a pseudo-Helmholtz configuration, with square coils separated by their side length. This resulted in a well-controlled field only in the immediate vicinity of the atom trap, with a limited volume of zero field. The modified apparatus makes use of three sets of square cross-section Helmholtz coils, whose ideal distance of separation was found using numerical modeling to be 0.55 times the side length. These coils produce an extended volume of zero magnetic field, allowing the atoms to experience free-fall for several hundred milliseconds. Under these conditions, the projected accuracy for measurements of g will be 0.5 ppb for a drop height of 30 cm. If the atoms are launched in a fountain, the experimental time scale can be further extended to 1 s.

We have also replaced the Ti:Sapphire laser with homebuilt, vacuum sealable, auto-locking diode laser systems (ALS) (Allan Deviation Floor 2×10^{-12} , output power 3 W) that can be stabilized to an atomic resonance without human intervention [11, 12]. Prototype lasers incorporated into industrial gravimeters have measured g at level of a 3 ppb and exceeded the performance specifications of commercial He-Ne lasers [11]. Accordingly, it is envisaged that the ALS will simultaneously operate the cold atom AI and an industrial gravimeter to systemic effects in the cold atom experiments.

3. RESULTS AND DISCUSSION

The excellent control of magnetic fields and field gradients in the phase 3 apparatus was recently demonstrated through a sensitive experiment for magnetic moment and magnetic state reconstruction of laser-cooled atoms [13]. Under these conditions, we have investigated methods of improving the grating contrast in the echo AI. We note the peak reflectivity in our previous measurements [2-5] has been limited to $\sim 0.1\%$. A possible approach for increasing the reflectivity is to preload cold atoms into a one-dimensional optical lattice [14] during the trapping phase using a sw pulse with a duration of several milliseconds. This approach has reported a fourfold enhancement in reflectivity by increasing the duration of the second sw pulse. We have developed a complementary approach [15] that characterizes the effect of the channeling of atoms during the formation of gratings due to matter wave interference following sw excitation. In this approach, we observe and model Pendellösung-like oscillations [16] in the backscattered signals as function of pulse width following (i)

excitation by a single sw pulse and (ii) excitation by two sw pulses resulting in echo formation. Our results indicate that the effect of channeling leads to a threefold improvement in the peak reflectivity without the need for lattice loading. We find that the increase in reflectivity can be achieved by increasing the duration of the relatively short first sw pulse. The increased reflectivity will make it feasible to investigate the sensitivity of echo AIs for measurements of g using the two-pulse and three-pulse geometries outlined in references [2, 3] as well as the frequency domain technique realized in reference [17].

4. ACKNOWLEDGEMENTS

We acknowledge helpful discussions with Louis Marmet of York University. This work was supported by the Canada Foundation for Innovation, the Ontario Innovation Trust, the Ontario Centers of Excellence, the Natural Sciences and Engineering Research Council of Canada (NSERC), York University, and the Helen Freedhoff Memorial Fund.

REFERENCES

- [1] B. Barrett, A. Carew, H. C. Beica, A. Vorozcovs, A. Pouliot, and A. Kumarakrishnan, *Atoms*, *4*, 19 (2016)
 - [2] C. Mok, B. Barrett, A. Carew, R. Berthiaume, S. Beattie, and A. Kumarakrishnan, *Phys. Rev. A* *88*, 023614, (2013)
 - [3] C. Mok, Demonstration of Improved Sensitivity of Echo Atom Interferometers to Gravitational Acceleration, *Ph.D. Thesis, York University, Toronto, Canada* (2013)
 - [4] B. Barrett, A. Carew, S. Beattie, and A. Kumarakrishnan, *Phys. Rev. A* *87*, 033626 (2013)
 - [5] B. Barrett, Techniques for Measuring the Atomic Recoil Frequency Using a Grating-Echo Atom Interferometer, *Ph.D. thesis, York University, Toronto, Canada* (2012)
 - [6] A. Carew, Apparatus for Inertial Sensing with Cold Atoms, *Ph.D. thesis, York University, Toronto, Canada* (2018)
 - [7] B. Barrett, L. Antoni-Micollier, L. Chichet, B. Battelier, P. A. Gominet, A. Bertoldi, P. Bouyer, and A. Landragin, *New J. Phys.* *17*, 085010 (2015)
 - [8] P. Cheinet, B. Canuel, F. Pereira Dos Santos, A. Gauguier, F. Yver-Leduc, and A. Landragin, *IEEE Trans.* *57*, 1141–1148 (2008)
 - [9] M. Kasevich, and S. Chu, *Phys. Rev. Lett.* *67*, 181(1991)
 - [10] A. Peters, K. Y. Chung, and S. Chu, *Nature* *400*, 849 (1999)
 - [11] H. C. Beica, A. Pouliot, A. Carew, A. Vorozcovs, N. Afkhami-Jeddi, T. Vacheresse, G. Carlse, P. Dowling, B. Barron, and A. Kumarakrishnan, *Review of Scientific Instruments.* *90*, 085113 (2019)
 - [12] A. Pouliot, H. C. Beica, A. Carew, A. Vorozcovs, G. Carlse, and A. Kumarakrishnan, *Proc. SPIE 10514, High-Power Diode Laser Technology XVI*, 105140S (2018)
 - [13] G. Carlse, A. Pouliot, T. Vacheresse, A. Carew, H. C. Beica, S. Winter, and A. Kumarakrishnan, *J. Opt. Soc. of Am. B* *37*, 1419 (2020)
 - [14] M. F. Andersen and T. Sleator, *Phys. Rev. Lett.* *103*, 070402, (2009)
 - [15] G. Carlse, J. Randhawa, A. Pouliot, T. Vacheresse, E. Ramos, and A. Kumarakrishnan, International Summer School in Quantum Technologies, Birmingham, UK (2023)
 - [16] R. D. Heidenreich, *Phys. Rev.* *62*, 5-6 (1942)
 - [17] M. Weel and A. Kumarakrishnan, *Phys. Rev A*, *67*, 061602(R) (2003)
- *akumar@yorku.ca; phone 1 416 736 2100 x77755; <http://datamac.phys.yorku.ca>